Cell Metabolism
Article

Cardiotrophin-1 Is a Key Regulator of Glucose and Lipid Metabolism

María J. Moreno-Aliaga,[1] Nerea Pérez-Echarri,[2,8] Beatriz Marcos-Gómez,[1,8] Eduardo Larequi,[2] Francisco Javier Gil-Bea,[3] Benoit Viollet,[4,5,6] Ignacio Gimenez,[7] J. Alfredo Martínez,[1] Jesús Prieto,[2,*] and Matilde Bustos[2,*]
[1]Department of Nutrition, Food Sciences, Physiology and Toxicology
[2]Division of Hepatology and Gene Therapy, Center for Applied Medical Research (CIMA)
[3]Department of Molecular Pharmacology (CIMA)
University of Navarra, 31008 Pamplona, Spain
[4]Inserm, U1016, Institut Cochin, 75014 Paris, France
[5]CNRS, UMR 8104, 75014 Paris, France
[6]Université Paris Descartes, 75014 Paris, France
[7]Department of Pharmacology and Physiology, University of Zaragoza, 50009 Zaragoza, Spain
[8]These authors contributed equally to this work
*Correspondence: jprieto@unav.es (J.P.), mbustos@unav.es (M.B.)
DOI 10.1016/j.cmet.2011.05.013

SUMMARY

Cardiotrophin-1 (CT-1) is a member of the gp130 family of cytokines. We observed that *ct-1*$^{-/-}$ mice develop mature-onset obesity, insulin resistance, and hypercholesterolemia despite reduced calorie intake. Decreased energy expenditure preceded and accompanied the development of obesity. Acute treatment with rCT-1 decreased blood glucose in an insulin-independent manner and increased insulin-stimulated AKT phosphorylation in muscle. These changes were associated with stimulation of fatty acid oxidation, an effect that was absent in *AMPKα2*$^{-/-}$ mice. Chronic rCT-1 treatment reduced food intake, enhanced energy expenditure, and induced white adipose tissue remodeling characterized by upregulation of genes implicated in the control of lipolysis, fatty acid oxidation, and mitochondrial biogenesis and genes typifying brown fat phenotype. Moreover, rCT-1 reduced body weight and corrected insulin resistance in *ob/ob* and in high-fat-fed obese mice. We conclude that CT-1 is a master regulator of fat and glucose metabolism with potential applications for treatment of obesity and insulin resistance.

INTRODUCTION

It has recently been shown that the balance between calorie procurement and disposal can be affected by gp130 receptor ligands including interleukin-6 (IL-6) and ciliary neurotrophic factor (CNTF). In particular, CNTF has been proposed as a potential therapy for obesity, glucose intolerance, and insulin resistance (Febbraio, 2007). This cytokine induces weight loss by hypothalamic control of energy balance (Janoschek et al., 2006) and improves glucose tolerance by activating skeletal muscle AMPK in chronic treatment (Watt et al., 2006). Notwithstanding these effects, *cntf* null mice have not been reported to develop obesity (Masu et al., 1993). The role of IL-6 in obesity and insulin resistance remains controversial. High circulating levels of IL-6 have been observed in obesity and are associated with the development of insulin resistance and type 2 diabetes, both in humans and rodents (Kristiansen and Mandrup-Poulsen, 2005; Tilg and Moschen, 2006). However, the discovery that IL-6 is a myokine (Febbraio et al., 2004) produced (Hiscock et al., 2004) and released (Steensberg et al., 2000) from skeletal muscle during exercise led many to challenge this concept, as insulin action is enhanced immediately after exercise (Wojtaszewski and Richter, 2006).

Cardiotrophin-1 (CT-1) is another member of the gp130 family of cytokines. We and others have previously reported that this cytokine is endowed with robust cytoprotective properties (Bustos et al., 2003; Iñiguez et al., 2006; Marquès et al., 2007; Pennica et al., 1996). Although it has been suggested that CT-1 might reduce insulin sensitivity in adipocytes (Zvonic et al., 2004), contributing to the development of the metabolic syndrome in humans (Natal et al., 2008), its role in lipid and glucose metabolism has not yet been characterized.

In this study, we examined the metabolic features of *ct-1* null mice and the effects on body composition, glucose, and lipid metabolism of acute and chronic administration of recombinant CT-1 (rCT-1). Our data reveal that CT-1 is a regulator of energy metabolism with potential applications in the treatment of obesity and the metabolic syndrome.

RESULTS

CT-1 Deficiency Is Associated with Adult-Onset Obesity, Dyslipidemia, and Insulin Resistance

ct-1 null and wild-type (WT) mice showed similar body weight at 2 months of age, but in the former group obesity was apparent at 6 months and progressed with time (Figures 1A and 1B). The analysis of body composition revealed that weight gain was mainly due to increased adipose tissue (Figure 1C). Body fat elevation was confirmed by weighing fat pads at different ages (Figure 1D). As expected, serum leptin levels augmented significantly in *ct-1*$^{-/-}$ mice in parallel with progression of adiposity (Figure 1E).

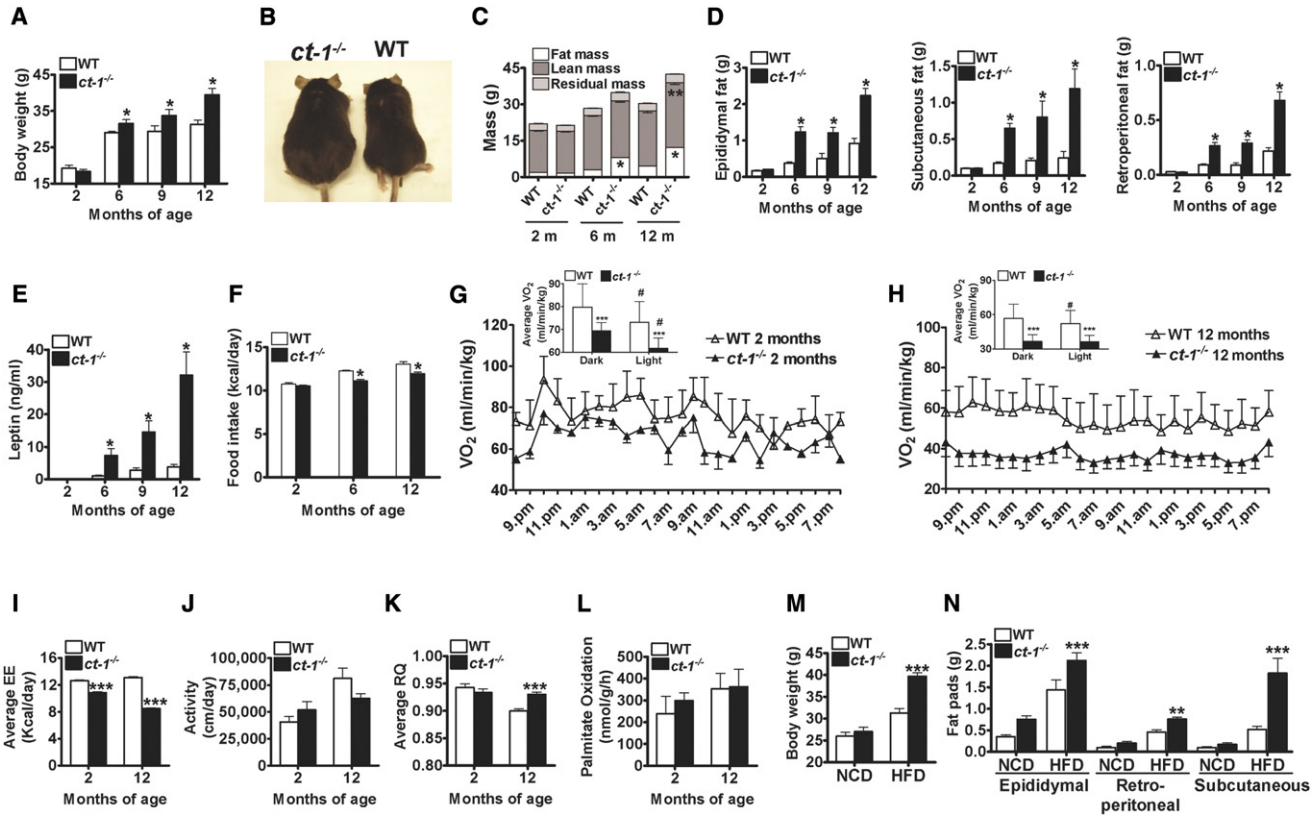

Figure 1. *ct-1*$^{-/-}$ Mice Develop Spontaneous Mature-Onset Obesity, and Young *ct-1*$^{-/-}$ Animals Exhibit Higher Susceptibility to Diet-Induced Obesity

(A) Body weight of wild-type (WT) (□) and *ct-1*$^{-/-}$ (■) male mice at various ages.

(B) Mice photographed at 12 months of age.

(C) Body composition of WT and *ct-1*$^{-/-}$ mice at different ages analyzed by QMR technology (see Experimental Procedures).

(D) Weights of three different fat pads (epididymal, subcutaneous, and retroperitoneal) from WT and *ct-1*$^{-/-}$ mice at different ages.

(E) Leptin levels in WT and *ct-1*$^{-/-}$ mice at different ages (n = 6).

(F) Food intake in WT and *ct-1*$^{-/-}$ mice at various ages (n = 11–13).

(G and H) Whole-body oxygen consumption rate (VO_2) during 24 hr in WT and *ct-1*$^{-/-}$ mice at 2 and 12 months of age (n = 4–8); #p < 0.05 represents differences between the dark and the light cycle.

(I) Average values of energy expenditure (EE) for the 24 hr period in WT and *ct-1*$^{-/-}$ mice at 2 and 12 months of age (n = 4–5).

(J) Physical activity for the 24 hr period in WT and *ct-1*$^{-/-}$ mice at 2 and 12 months of age (n = 4–5).

(K) Average respiratory quotient (VCO_2/VO_2) (RQ) for the 24 hr period in WT and *ct-1*$^{-/-}$ mice at 2 and 12 months of age (n = 4–5).

(L) Fatty acid oxidation in soleus muscle in WT and *ct-1*$^{-/-}$ mice at 2 and 12 months of age (n = 5).

(M and N) Body and fat pat weights of young WT and *ct-1*$^{-/-}$ mice (5 months old) fed with NCD (normal chow diet) and HFD (high-fat diet) for 12 weeks (n = 5–8).

Results are means ± SEM; *p < 0.05, **p < 0.01, ***p < 0.001 between WT and *ct-1*$^{-/-}$ mice. (See also Figure S1 and Table S1.)

Longitudinal analysis of food intake from 2 to 12 months showed that *ct-1*$^{-/-}$ mice became obese despite reduced food intake (Figure 1F), suggesting that energy expenditure (EE) could be altered in these animals. Indeed, in 2-month-old *ct-1* null mice, oxygen consumption and EE were significantly reduced in comparison with WT mice of the same age, and these differences increased in old animals (Figures 1G–1I). The differences in oxygen consumption observed in 12-month-old mice (Figure 1H) were also prominent after normalizing by lean mass (73.55 ± 0.87 versus 54.25 ± 0.58 ml/min/kg lean mass, p < 0.001). Changes in EE were not attributable to physical activity (Figure 1J) nor to differences in BAT mass or expression in BAT of genes involved in thermogenesis (data not shown), which were similar in *ct-1*$^{-/-}$ and WT mice at 2 months. Thus, our data indicate that decreased EE precedes the development of obesity in *ct-1* null mice.

Notably, the respiratory quotient (RQ) was significantly elevated in mature obese *ct-1*$^{-/-}$ mice (Figure 1K), a finding that was suggestive of reduced fat utilization. We found that the fatty acid oxidative capacity of isolated skeletal muscle (as estimated by the production of $^{14}CO_2$ from [U-^{14}C]palmitate) was comparable in WT and *ct-1* null mice (Figure 1L). Thus, it seems possible that the increase in RQ might be due to impaired lipid mobilization. This concept is in agreement with the presence of lower circulating free fatty acids in old obese *ct-1*-deficient mice (see Table S1 available online).

CT-1 deficiency strongly predisposes to obesity, as shown by the fact that 2-month-old *ct-1*$^{-/-}$ mice exposed for 12 weeks to

a high-fat diet (HFD) gained more weight and accumulated more epididymal, retroperitoneal, and subcutaneous fat mass than WT animals (Figures 1M and 1N). Remarkably, *ct-1*$^{-/-}$ mice recapitulate many of the features of the human metabolic syndrome, including hypercholesterolemia, hyperglycemia, and hyperinsulinemia (Table S1), alterations that were observed from 6 months onward. Moreover, when young animals were exposed to HFD, *ct-1* null mice, but not WT animals, experienced a marked increase in basal glycemia (212.4 ± 26.5 versus 110.80 ± 6.01 mg/dl, $p < 0.05$), insulinemia (2.08 ± 0.76 versus 0.58 ± 0.12 ng/ml, $p < 0.05$), and total cholesterol (314.8 ± 22.3 versus 158.0 ± 7.03 mg/dl, $p < 0.001$), reflecting the decisive influence of CT-1 on glucose and lipid metabolism. In *ct-1*$^{-/-}$ mice on a normal chow diet, pancreatic islet number and size were increased at 9 and 12 months (Figure S1A), and the insulin tolerance test (ITT) was already altered at 6 months (Figure S1B). In agreement with these findings, insulin-stimulated AKT phosphorylation was reduced in both skeletal muscle and WAT of 6-month-old *ct-1*$^{-/-}$ animals (Figure S1C). These disturbances were not present in nonobese 2-month-old *ct-1* null mice (Figures S1D and S1E), indicating that insulin resistance in CT-1 deficiency is obesity dependent.

Reduced Expression of Lipolytic Genes and Impaired Mitochondrial Biogenesis in WAT from Obese *ct-1*-Deficient Mice

Mature *ct-1*$^{-/-}$ mice showed adipocyte hypertrophy (Figure S1F). In WAT from these animals, there was a significant reduction in the expression of adipose triglyceride lipase (*ATGL*) and hormone-sensitive lipase (*HSL*), which are key executors of the hydrolysis of triglycerides (TG) and diglycerides (Figure S1G). Isolated adipocytes from 2-month-old *ct-1*-deficient mice showed no differences in basal and isoproterenol-induced lipolysis when compared with WT adipocytes. In contrast, adipocytes from old obese *ct-1* null mice responded poorly to isoproterenol, although baseline lipolysis was increased (Figure S1H), as reported for hypertrophic adipocytes (Wueest et al., 2009).

Genes involved in mitochondrial biogenesis, including peroxisome proliferator-activated receptor-γ coactivator-1α (*PGC-1*α) and endothelial nitric oxide synthase (*eNOS*), were downregulated in WAT from obese, but not young, *ct-1*$^{-/-}$ mice (Figure S1I). In addition, mitochondrial DNA levels were reduced in WAT from old *ct-1*$^{-/-}$ mice compared with WT animals (Figure S1J). Furthermore, oxygen consumption was reduced in isolated adipocytes from old obese *ct-1* null mice, while this was not observed in adipocytes from young animals (Figure S1K). Altogether, our findings suggest that the observed changes in lipolysis and mitochondrial biogenesis are secondary to obesity and insulin resistance.

ct-1 Is a Nutritionally Regulated Gene: Effects of Chronic CT-1 Treatment on Adipocyte Size, Fatty Acid Oxidation, and WAT Remodeling

Since CT-1 deficiency leads to marked derangement in fuel homeostasis, we asked whether CT-1 could be a nutritionally regulated gene. In epididymal WAT we observed that *ct-1* mRNA expression increased markedly when mice were subjected to 48 hr fast and decreased promptly upon refeeding. Similar changes were observed in skeletal muscle, liver, and heart in response to fasting and refeeding (Figure S2A), indicating that CT-1 is regulated by nutritional status.

On the basis of these findings, we investigated the metabolic effects induced by chronic treatment with rCT-1. We found that intravenous (i.v.) administration of rCT-1 (0.2 mg/kg/day) for 6 days to 24-week-old male WT mice caused a significant reduction in body weight (Figure 2A) and food intake (10.88 ± 0.51 versus 7.36 ± 0.96 kcal/day per mouse, $p < 0.01$). rCT-1-treated mice lost significantly more weight than pair-fed (PF) animals (Figure 2A), indicating that CT-1 enhanced energy utilization besides reducing food intake. The doses of rCT-1 used in this study were comparable to those of CNTF able to reduce food intake and body weight (Lambert et al., 2001; Steinberg et al., 2006). After rCT-1 injection serum levels were considerably above physiological values (~2 μg/ml at 10 min after injection), the estimated rCT-1 half-life being 1.17 hr. Similarly to other anorexigenic cytokines (Lambert et al., 2001), rCT-1 induced a hypophagic response when given by either i.v. or intracerebroventricular (i.c.v.) injection. Accordingly, we could observe activation of hypothalamic pathways involved in hypophagia, including signal transduction activator of transcription 3 (STAT-3) and S6 ribosomal protein (S6), 45 minutes after i.v. or i.c.v. administration of rCT-1 (Figure S2B).

To further elucidate the mechanisms underlying the slimming properties of CT-1, we analyzed WAT histology and gene expression in normal mice receiving saline, in mice treated with rCT-1, and in PF animals. We found that the average adipocyte size was smaller in rCT-1-treated animals even when compared with the PF group (Figure 2B). Reduced adipocyte size correlated with decreased expression of the lipogenic genes such as fatty acid synthase (*FAS*), adipocyte determination and differentiation-dependent factor 1 (*ADD1*), sterol CoA desaturase 1 (*SCD1*), and acetyl CoA carboxylase-α (*ACC*α) (Figure 2C). Furthermore, mice given rCT-1 therapy showed increased expression of the lipolytic genes *HSL* and *ATGL* compared with PF (Figure 2C).

In addition to regulating lipogenic and lipolytic genes, CT-1 seems to be able to modulate fat utilization in WAT. This was suggested by the fact that two genes involved in fatty acid oxidation, namely carnitine palmitoyl transferase I (*CPT-1*) and acyl-CoA oxidase (*ACO*), were upregulated in WAT from rCT-1-treated mice compared with PF group (Figure 2C). Consistent with these data, fatty acid oxidation in WAT from rCT-1-treated mice was increased as compared with PF group (Figure 2D). Moreover, a direct stimulatory effect of rCT-1 on fatty acid oxidation was also observed when adipose tissue fragments were incubated with this cytokine (Figure S2C). Also, mitochondrial biogenesis was enhanced in WAT from mice treated with rCT-1 compared with PF animals. This was reflected by (1) upregulation of genes implicated in the control of mitochondrial function and regulation of BAT (*PGC-1*α, transcription factor A mitochondrial [*TFAM*], *NRF1*, *eNOS*, uncoupling protein [*UCP*] *2*, *UCP1*, *PRDM16*, and deiodinase iodothyronine type II [*Dio2*]) (Figure 2E), (2) increased content of the mtDNA-encoded COX1, (3) higher mitochondrial mass as estimated by MitoTracker Green FM labeling, and (4) increased oxygen consumption by isolated adipocytes of animals given rCT-1 (Figures 2F–2H). In vitro studies using 3T3-L1 adipocytes showed that

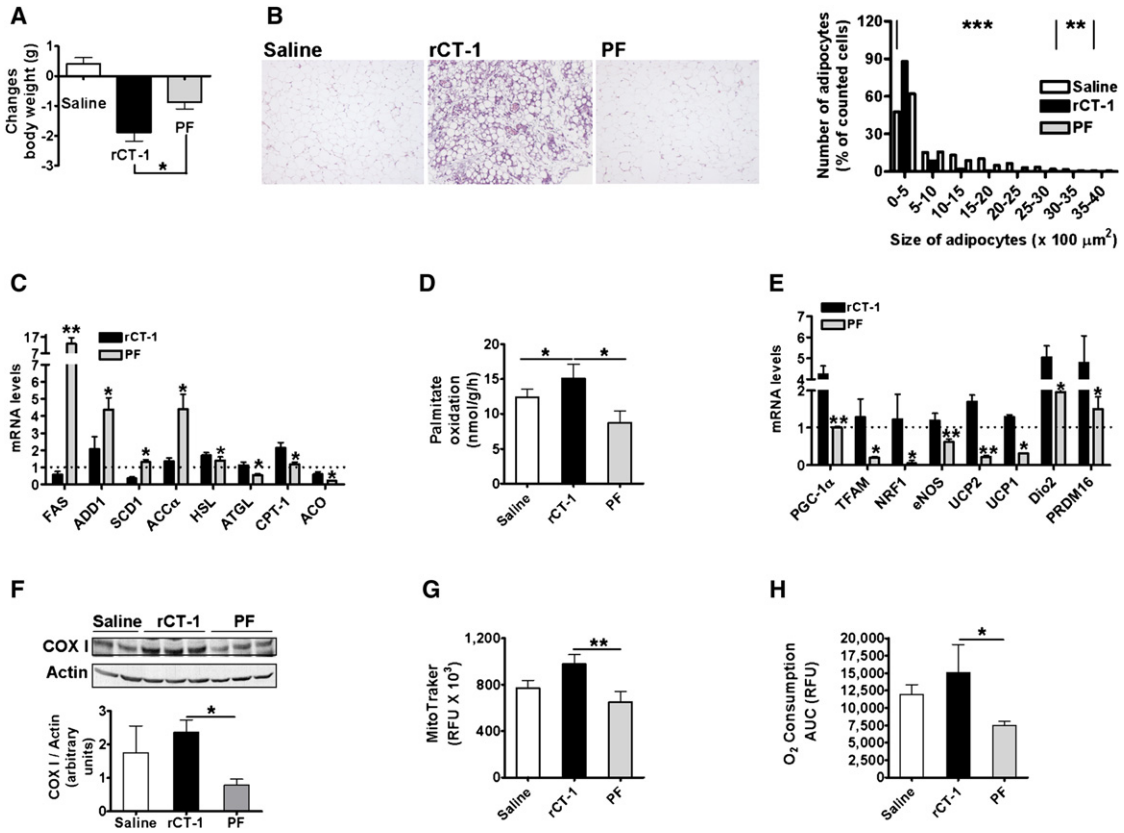

Figure 2. Chronic Exposure to rCT-1 Decreases Body Weight and Induces a Marked Metabolic Remodeling in WAT

(A) Body weight changes after daily rCT-1 i.v. treatment (0.2 mg/kg/day) for 6 days in 24-week-old WT mice in comparison to saline-treated control mice fed ad libitum and saline-treated mice pair-fed (PF) to the amount of food consumed by the rCT-1-treated group (n = 6).

(B) H&E-stained (100×) paraffin-embedded sections of epididymal WAT from saline, rCT-1-treated animals, and PF group. Distribution of adipocyte size.

(C) Relative expression of genes encoding key factors in lipogenesis, lipolysis, and fatty acid oxidation in epididymal WAT from saline, rCT-1-treated, and PF mice. Data are expressed as fold change relative to saline-treated control mice fed ad libitum considered as 1 (dotted line) (n = 6).

(D) Fatty acid oxidation in epididymal fat from saline, rCT-1-treated animals, and PF mice (n = 5).

(E) Relative mRNA levels of genes involved in mitochondrial biogenesis and brown adipose tissue-specific genes in WAT of saline (considered as 1), rCT-1-treated, and PF mice (n = 6).

(F) Representative western blot and densitometric analysis of COX1 in WAT from saline, rCT-1-treated, and PF mice.

(G) Epididymal adipocytes isolated from rCT-1-treated mice contain more mitochondria, as indicated by MitoTracker labeling. Data are presented as area under curve (AUC) of RFU (relative fluorescent units) normalized by 10^6 cells (n = 8–11).

(H) Oxygen consumption in adipocytes from saline, rCT-1-treated, and PF group. Data are presented as area under curve (AUC) of RFU (relative fluorescent units) normalized by 10^6 cells (n = 10). Results are means ± SEM; *p < 0.05, **p < 0.01, ***p < 0.001 PF versus rCT-1-treated group. (See also Figure S2.)

CT-1, but not CNTF, was able to upregulate *Dio2* and *UCP1*, two BAT characteristic genes (Figure S2D).

CT-1 Increases Fatty Acid Oxidation in Muscle

To test whether the body-weight-lowering activity of CT-1 is accompanied by a stimulatory effect on fat utilization, we determined RQ changes in the fasting state after a single i.v. dose of rCT-1 (10 μg/mouse). Mice receiving rCT-1 showed a significant reduction of mean RQ compatible with activation of fatty acid oxidation (Figure 3A) and exhibited, at 3 hr after rCT-1 injection, marked upregulation of skeletal muscle genes involved in this process, namely *PGC-1β*, *ACO*, acyl-CoA dehydrogenase (*ACD*), and medium-chain acyl-CoA dehydrogenase (*MCAD*) (Figure 3B). To confirm that CT-1 might enhance fat utilization, we fed animals with a high-fat/sucrose meal while injecting i.v. a single dose of rCT-1 (10 μg/mouse) or saline, and RQ was measured over the following 8 hr. We found that RQ was lower in rCT-1-treated mice than in controls (Figure 3C), indicating stimulation of postprandial FFA oxidation. In addition, after a high-fat/sucrose meal, saline-treated animals showed the expected postprandial rise in plasma FFA and TG, while in those receiving rCT-1 serum, TG failed to increase, and serum FFA experienced a rapid and pronounced decline after the meal (Figure 3D). To rule out decreased fat absorption as responsible for these postprandial changes in serum lipids, we administered an intravenous bolus of Lipofundin (a lipid emulsion), and the decay of plasma FFAs after the injection was monitored in mice treated 30 min before with either rCT-1 (10 μg/mouse) or saline. We observed that rCT-1 caused a marked acceleration in the removal of FFAs from plasma (Figure 3E).

AMPK is considered to be a master regulator of fatty acid oxidation (Viollet et al., 2009). We found that acute administration

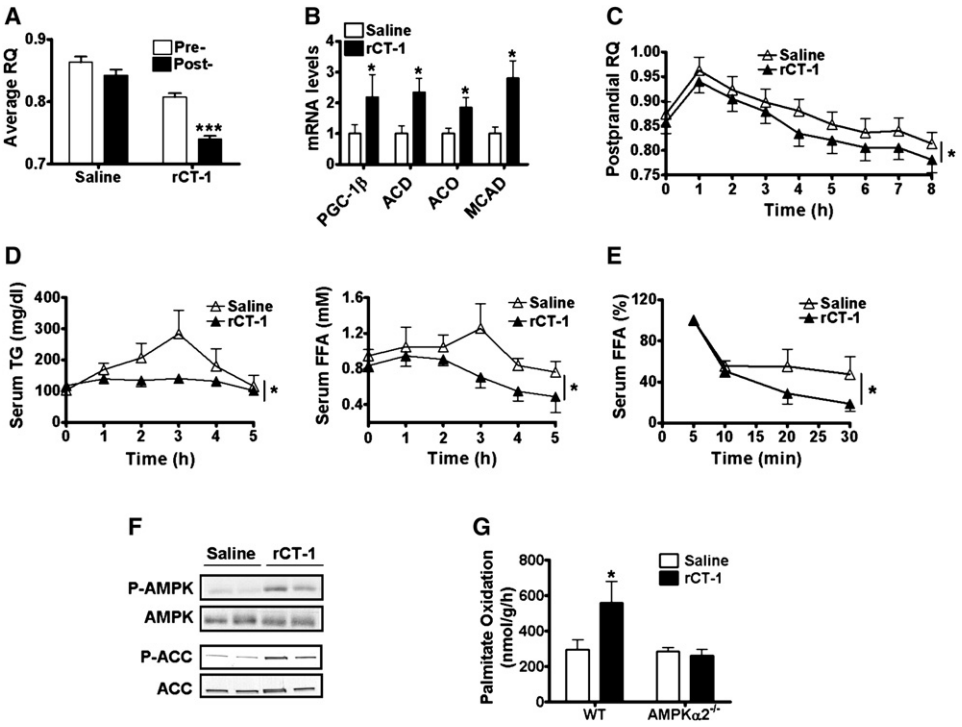

Figure 3. Effects of Acute Treatment with rCT-1 on Energy and Lipid Metabolism

(A) Average respiratory quotient (RQ) pre- and post-rCT-1 administration (10 μg/mouse, i.v.) to fasted WT mice. After a 14 hr acclimation period, VO_2 and VCO_2 were measured during 3–4 hr. After confirming the stability of RQ, rCT-1 or saline was administered and calorimetry was performed during 6 hr (n = 5).

(B) Peroxisome proliferator-activated receptor-γ coactivator-1β (*PGC-1β*), acyl-CoA dehydrogenase (*ACD*), acyl-CoA oxidase (*ACO*), and medium-chain acyl-CoA dehydrogenase (*MCAD*) mRNA levels in skeletal muscle 3 hr after rCT-1 administration (n = 5).

(C) RQ after a high-fat/sucrose meal given by gavage in saline and rCT-1-treated WT mice (n = 9–12).

(D) Effect of rCT-1 on serum FFA and TG levels in WT mice after a high-fat/sucrose meal (n = 5).

(E) rCT-1 treatment accelerates the removal of serum FFAs. Five minutes after Lipofundin injection, FFA levels raised from 0.73 ± 0.05 to 2.25 ± 0.31 mM in saline-treated animals and from 0.70 ± 0.08 to 2.62 ± 0.49 mM in rCT-1-treated animals. Clearance of FFA from serum measured at later time points was normalized to FFA levels at 5 min after Lipofundin injection (100%). Statistical analyses for (C)–(E) were performed by repeated-measures two-way ANOVA with Bonferroni posttest (*$p < 0.05$).

(F) Phospho-AMPK (Thr172) and phospho-ACC (Ser79) signaling in skeletal muscle at 1 hr after a single dose of rCT-1 in fasted WT mice (n = 5).

(G) Palmitate oxidation in isolated skeletal muscle from WT and *AMPKα2*$^{-/-}$ mice in the absence or presence of rCT-1 (20 ng/ml) (n = 5). Results are means ± SEM; *$p < 0.05$, ***$p < 0.001$. (See also Figure S3.)

of rCT-1 stimulated the phosphorylation of AMPK and its downstream target ACC in skeletal muscle (Figure 3F). Moreover, palmitate oxidation was significantly increased in isolated soleus muscle incubated with rCT-1 as compared with contralateral muscle incubated with saline (Figure 3G). Since in skeletal muscle the actions of AMPK are thought to be mediated mainly through the AMPKα2 isoform (Wojtaszewski et al., 2002), we performed palmitate oxidation in the soleus muscle from *AMPKα2*$^{-/-}$ mice in the presence or absence of rCT-1. We found that rCT-1 treatment increased palmitate oxidation only in WT but not in *AMPKα2*$^{-/-}$ mice, indicating that AMPK α2 is essential for rCT-1 to stimulate fatty acid oxidation (Figure 3G).

Leptin has been shown to induce the expression of genes involved in fatty acid oxidation through central activation (Minokoshi et al., 2002). In order to investigate whether rCT-1 could exert similar effects, we placed a cannula into the lateral ventricle of C57BL/6 mice and injected rCT-1 (1 μg) or saline i.c.v. At 6 hr after infusion, we found no change in mRNA levels of *PGC-1β*, *ACO*, *ACD*, or *MCAD* in skeletal muscle (Figure S3), signifying that rCT-1 modulates fatty acid oxidation mainly by peripheral effects.

CT-1 Regulates Glucose Homeostasis

The effect of CT-1 on glucose homeostasis was analyzed by determining plasma glucose and insulin 1 hr after a single i.v. dose of rCT-1 (10 μg/mouse) or saline to WT mice. We detected a significant decrease of plasma glucose without changes in insulin levels following rCT-1 administration (Figure 4A). The insulin-sensitizing activity of CT-1 was associated with activation of AKT in skeletal muscle of rCT-1-treated mice (Figure 4B). The effect of CT-1 in facilitating the action of insulin was also confirmed by injecting rCT-1 (10 μg/mouse) 30 min before performing an ITT in 6-month-old WT mice. rCT-1 was able to decrease significantly the rise in glucose concentrations during the rebound phase of the test (Figure 4C). The glycemia-lowering properties of rCT-1 were confirmed in two additional models. In animals given a high-fat/sucrose meal, the administration of rCT-1 significantly decreased postprandial plasma glucose levels (Figure 4D). Moreover, in mice with streptozotocin (STZ)-induced insulin deficiency, the administration of rCT-1 caused a significant fall in plasma glucose (Figure 4E), demonstrating an insulin-independent effect of CT-1 on glucose homeostasis.

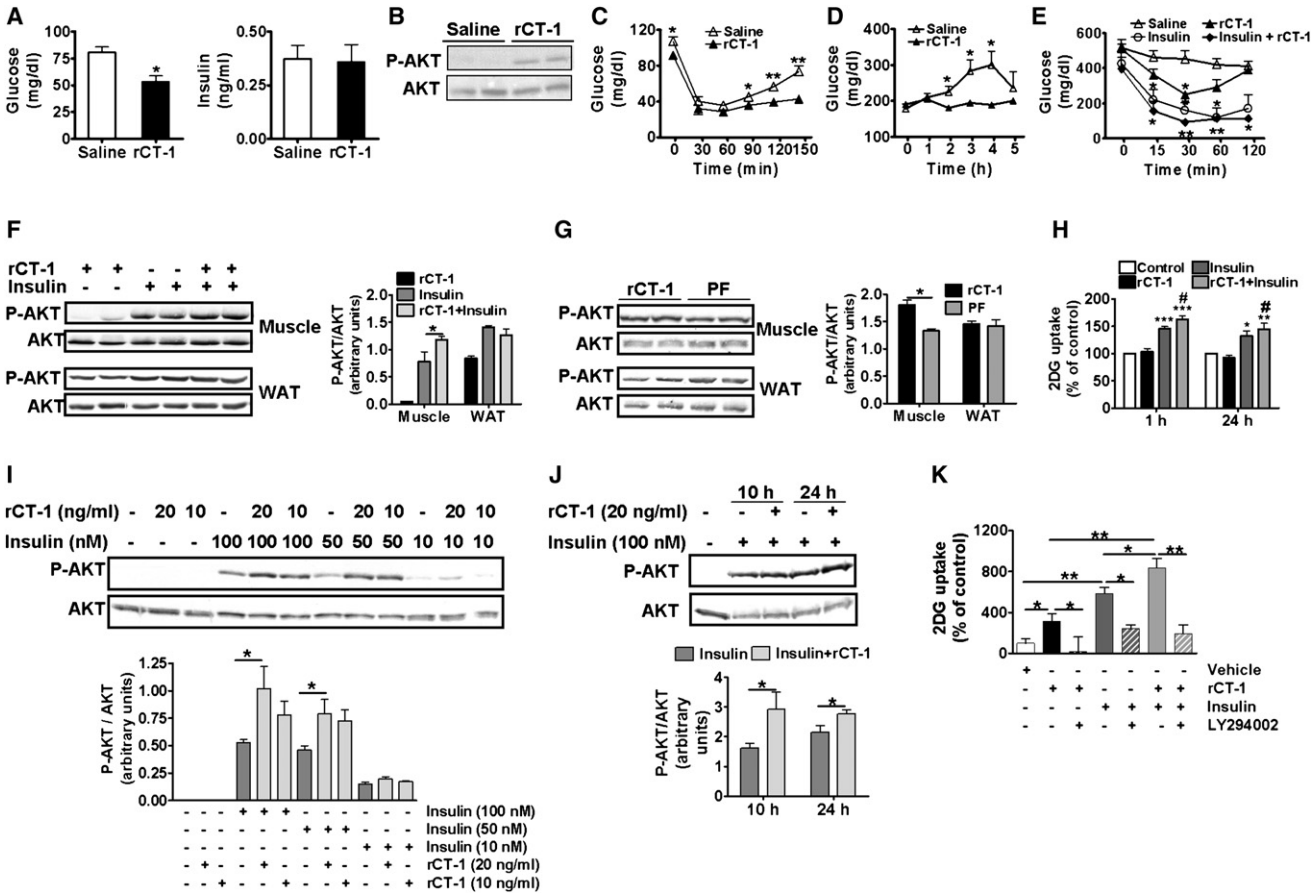

Figure 4. Glucose-Lowering Effects of rCT-1 in Different Models

(A) rCT-1 modifies insulin signaling in muscle and adipose tissue. Glucose and insulin levels at 1 hr after a single dose of rCT-1 (10 μg/mouse) in fasted WT mice (n = 5).

(B) Ser473-phosphorylated AKT (P-AKT) in skeletal muscle in the same animals.

(C) ITT in WT mice (6 month s old) injected with rCT-1 (n = 5).

(D) Effect of rCT-1 on serum glucose levels after a high-fat/sucrose meal (n = 4).

(E) Changes in glucose levels in STZ-treated mice after the injection of rCT-1, insulin, or both (n = 5).

(F) Fasted WT mice were injected with saline or rCT-1 for 30 min, then insulin (0.5 U/mouse) was injected through the inferior vena cava. P-AKT signaling in skeletal muscle and WAT was assessed by immunoblot analysis and quantified by densitometry (n = 5).

(G) P-AKT signaling in muscle and WAT from rCT-1 (0.2 mg/kg/day) or saline (PF)-treated animals for 6 days, fasted for 16 hr, and injected with insulin (0.5 U/mouse) in the inferior vena cava (n = 5).

(H) rCT-1 effects on 2-deoxyglucose (2DG) uptake in L6E9 myotubes in the absence or presence of insulin (n = 6); *p < 0.05, **p < 0.01, ***p < 0.001 versus control cells, and #p < 0.05 versus insulin-treated cells.

(I and J) Representative western blots and densitometric analysis of P-AKT signaling in L6E9 myotubes treated with rCT-1 and insulin for 15 min or pretreated with rCT-1 (20 ng/ml) for 10 and 24 hr and stimulated with insulin for 5 min.

(K) Effect of AKT inhibitor LY294002 (50 μM) on 2DG uptake in isolated soleus muscle incubated with 20 ng/ml of rCT-1 (30 min) in the absence or presence of insulin (100 nM). Results are means ± SEM; *p < 0.05, **p < 0.01. (See also Figure S4.)

In addition, we found that treatment with rCT-1 (10 μg/mouse) 30 min prior to insulin stimulation (0.5 U/mouse injected through the inferior vena cava) resulted in increased insulin-induced AKT phosphorylation in muscle but not in adipose tissue (Figure 4F). Similarly, we observed stronger insulin-induced AKT phosphorylation in skeletal muscle in animals subjected to chronic administration of rCT-1 (0.2 mg/kg/day) for 6 days compared with PF mice given saline (Figure 4G). To better characterize the role of CT-1 in regulating insulin sensitivity in skeletal muscle, we performed in vitro studies in L6E9 myotubes. Our data showed that acute (1 hr) and chronic (24 hr) treatment with rCT-1 significantly increased insulin-stimulated glucose uptake (Figure 4H) as well as AKT phosphorylation (Figures 4I and 4J) in these cells. Furthermore, using isolated soleus muscle, we demonstrated that AKT is a major mediator in the stimulatory effect of rCT-1 in glucose uptake by muscle (Figure 4K). We also examined the ability of rCT-1 to regulate insulin signaling and glucose uptake in fully differentiated 3T3-L1 adipocytes. In the absence of insulin, rCT-1 treatment was able to activate AKT phosphorylation and to increase baseline glucose uptake. Treatment with rCT-1 (24 hr) also increased insulin-stimulated glucose uptake. The inhibition of AKT blocked these effects (Figure S4).

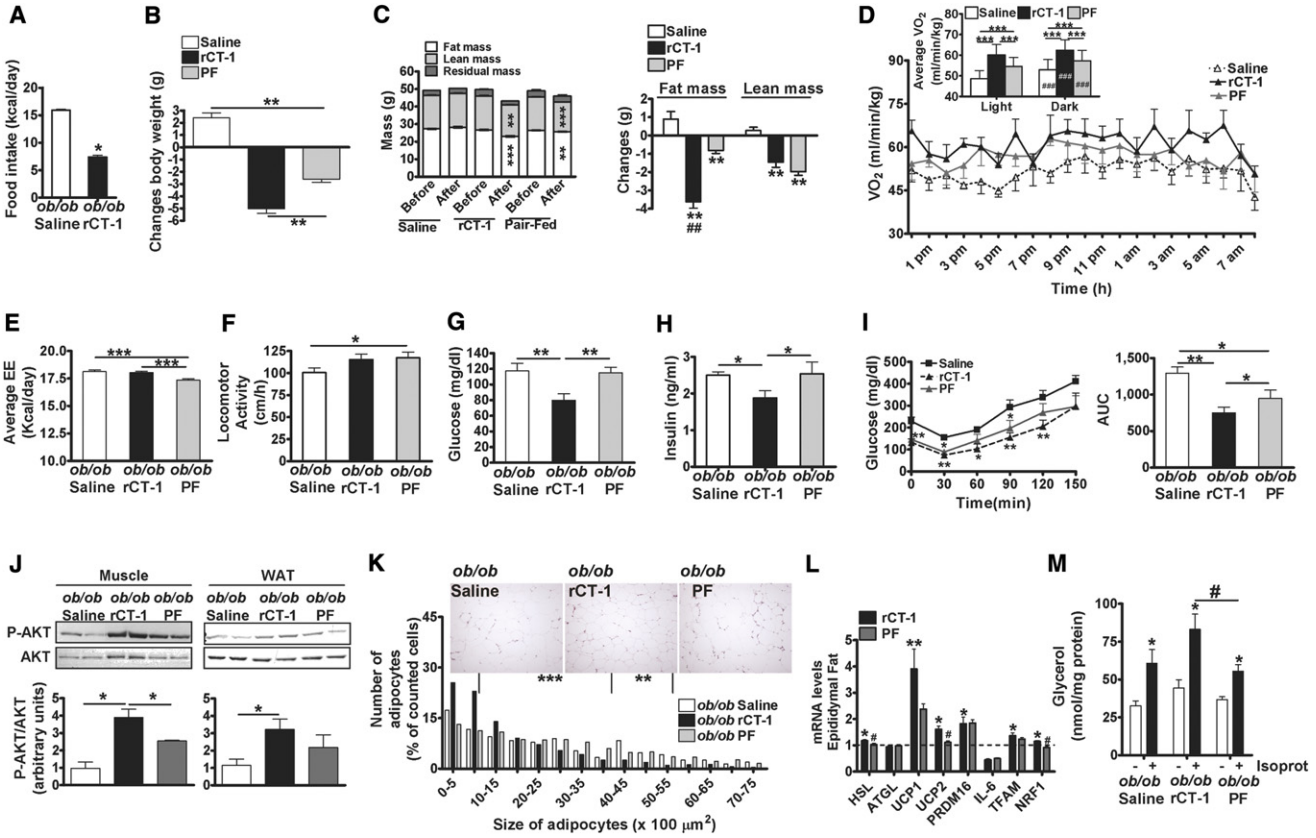

Figure 5. Chronic rCT-1 Treatment Reduces Fat Mass and Corrects Insulin Resistance in Genetic Model of Obesity

(A–C) Changes in daily food intake (A), body weight (B), and body composition (C) (left panel) in *ob/ob* mice before and after treatment with rCT-1 (0.2 mg/kg/day) or saline (ad libitum controls and PF) during 10 days (n = 6–7); **p < 0.01 and ***p < 0.001, before versus after. Changes in body composition in these animals (right panel); **p < 0.01 versus saline and ##p < 0.01 rCT-1 versus PF.

(D–F) Whole-body oxygen consumption rate (VO_2), energy expenditure, and physical activity in rCT-1-treated *ob/ob* mice at the end of the treatment. ###p < 0.001 represents differences between the dark and the light cycle.

(G and H) Serum glucose (G) and insulin levels (H) in saline, rCT-1-treated, and PF *ob/ob* mice.

(I) Insulin tolerance test (ITT) in saline, rCT-1-treated, and PF *ob/ob* mice (n = 5–6).

(J) Representative western blots and densitometric analysis of insulin-stimulated P-AKT (Ser473) in skeletal muscle and epididymal WAT from saline, rCT-1-treated, and PF *ob/ob* mice.

(K) H&E-stained paraffin-embedded sections of epididymal WAT from saline, rCT-1-treated, and PF *ob/ob* mice. Distribution of adipocyte size (n = 5–6); **p < 0.01 and ***p < 0.001 versus PF.

(L) Relative mRNA levels of *HSL*, *ATGL*, *UCP1*, *UCP2*, *PRDM16*, *il-6*, *TFAM*, and *NRF1* in epididymal WAT from rCT-1-treated *ob/ob* mice in comparison to saline and PF-treated mice. Data are expressed as fold change relative to saline-treated control considered as 1 (dotted line) (n = 5–6); *p < 0.05, **p < 0.001 versus saline-treated group, and #p < 0.05 versus rCT-1-treated group.

(M) Basal and isoproterenol-stimulated lipolysis measured by glycerol release in adipocytes isolated from epididymal WAT of saline, rCT-1-treated, and PF *ob/ob* mice (n = 4). Results are means ± SEM; *p < 0.05 versus basal (isoproterenol-untreated) adipocytes and #p < 0.05 rCT-1 versus PF in isoproterenol-treated adipocytes. (See also Figure S5 and Table S2.)

Recombinant CT-1 Reduces Adiposity and Corrects Insulin Resistance in Genetic and Acquired Models of Obesity

We then asked whether rCT-1 therapy could reduce adiposity in a genetic model of obesity. To this end we administered rCT-1 (0.2 mg/kg/day) i.v. to *ob/ob* mice for 10 days. We observed that this treatment reduced food intake and significantly diminished body weight and fat mass compared with both mice injected with saline and PF animals (Figures 5A–5C). Interestingly, rCT-1-treated mice experienced less loss of lean mass and more pronounced decrease of fat stores than the PF group (Figure 5C). Also, whole-body O_2 consumption was significantly increased in rCT-1-treated animals as compared with saline and PF groups (Figure 5D). Consonant with the reduction of food intake, PF animals exhibited an adaptive reduction of EE, which was not observed in mice receiving rCT-1 (Figure 5E). Differences in oxygen consumption could not be ascribed to variations in physical activity, which was similar in saline and rCT-1 treated groups (PF group exhibited increased locomotor activity due to "food seeking behavior") (Figure 5F). Neither BAT mass nor mRNA levels of *UCP1* (a key thermogenic molecule) in BAT showed differences among groups (Figure S5A).

Importantly, in rCT-1-treated mice, we observed a significant reduction in glycemia and insulinemia together with a significant

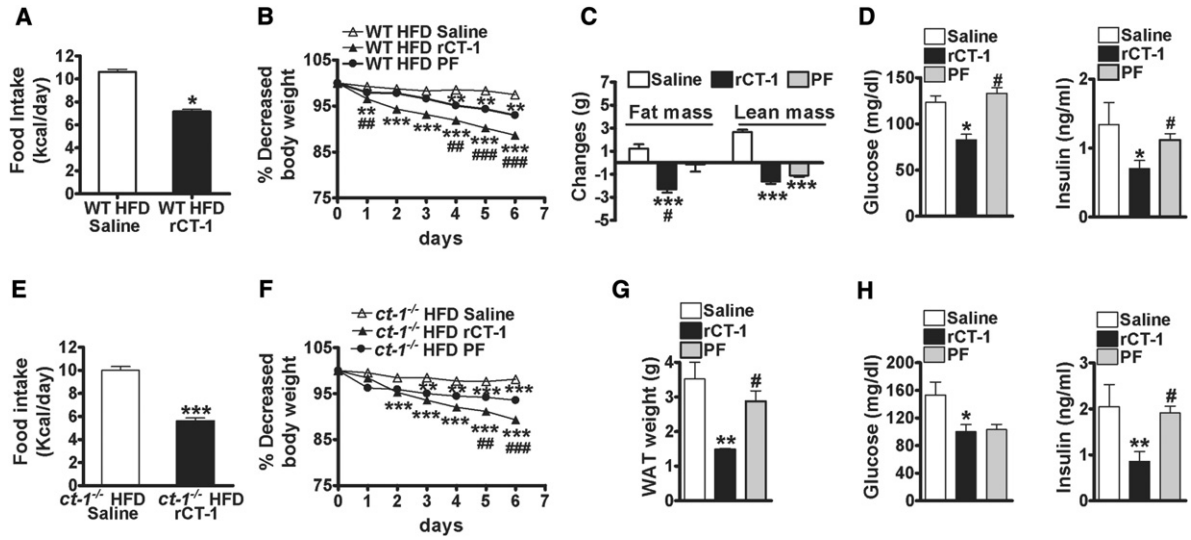

Figure 6. Chronic rCT-1 Treatment Decreases Body Weight, Fat Mass, Glucose, and Insulin Levels in HFD-Fed WT and *ct-1* Null Mice

(A–D) Changes in food intake (A), body weight (B), body composition (C), and serum glucose and insulin levels (D) in rCT-1-treated HFD-fed WT mice.

(E–H) Changes in food intake (E), body weight (F), and WAT weights (G) estimated by the sum of epididymal, retroperitoneal, and subcutaneous depot weights and serum glucose and insulin levels in rCT-1-treated HFD-fed *ct-1*$^{-/-}$ mice (H). Animals were fed on HFD for 12 weeks followed by 6 days treatment with rCT-1 (0.2 mg/kg/day) or saline (control or PF) (n = 5–10). Data are means ± SEM; *p < 0.05, **p < 0.01, ***p < 0.001 versus saline-treated mice. #p < 0.05, ##p < 0.01, ###p < 0.001 versus PF group. (See also Table S3.)

improvement in ITT as compared with both saline and PF groups (Figures 5G–5I), indicating improvement of insulin sensitivity in mice given rCT-1. This was confirmed in an additional study where animals were sacrificed 5 min after insulin administration (1 U/g). We found a significant increase of AKT phosphorylation in muscle in rCT-1-treated mice as compared with the other groups. However, no significant differences were found in AKT phosphorylation in WAT between mice receiving rCT-1 and PF group (Figure 5J). In addition to the glucose-lowering effect, rCT-1 therapy was associated with reduction of total and LDL cholesterol while TG levels increased, possibly due to fat mobilization (Table S2).

On histological examination, epididymal WAT from *ob/ob* mice treated with rCT-1 showed smaller adipocytes (Figure 5K), a finding that was accompanied by upregulation of *HSL*, *UCP2*, and *NRF1* compared with PF group. Moreover, upregulation of *UCP1*, *TFAM*, and *PRDM16* in concert with downregulation of *il-6* was observed in rCT-1-treated and PF groups compared with controls receiving saline (Figure 5L). A similar gene expression pattern was observed in subcutaneous fat (Figure S5B). To further assess the influence of rCT-1 on fat mobilization, we determined glycerol release from isolated *ob/ob* adipocytes obtained from the three experimental groups. Our data showed that adipocytes from rCT-1-treated mice exhibited increased lipolytic response to isoproterenol as compared with PF group (Figure 5M). Interestingly, treatment with rCT-1 was accompanied by a significant reduction of proinflammatory mediators including IL-6, MCP-1, resistin, and t-PAI in serum (Table S2) and by absence of changes in rectal temperature (data not shown). Moreover, rCT-1 treatment was not followed by a rebound of accelerated weight recovery. Weight gain after cessation of the therapy was comparable in rCT-1 and PF groups, and both responded similarly to a new course of treatment (Figure S5C).

To determine if rCT-1 could ameliorate weight gain and restore insulin sensitivity in an acquired model of obesity, we administered saline or rCT-1 i.v. (0.2 mg/kg/day) during 6 days to WT and *ct-1* null mice receiving HFD for 12 weeks. Also in these models, we found that treatment with rCT-1 significantly decreased food intake and diminished body weight, fat mass, and hyperinsulinemia as compared with PF group (Figure 6 and Table S3).

DISCUSSION

Our data show that CT-1 is a key cytokine controlling energy balance. Mice lacking CT-1 develop adult-onset obesity, accompanied by hyperglycemia, hyperinsulinemia, and hypertrophy of pancreatic islets mimicking type 2 diabetes. The similarity of *ct-1*-deficient mice to the human metabolic syndrome also extends to the presence of dyslipidemia with increased total and LDL cholesterol. In *ct-1* null mice, the development of obesity and the metabolic syndrome is preceded by decreased EE. This defect is already present in young nonobese animals and becomes more severe with aging. Our data clearly show that CT-1 deficiency predisposes to obesity and dyslipidemia from the early ages of life, as shown in young *ct-1* null mice when subjected to HFD. In keeping with a function of CT-1 as a regulator of energy metabolism, we observed that *ct-1* mRNA is upregulated during fasting and downregulated by refeeding in WAT, liver, and muscle, indicating that CT-1 behaves as a nutrient sensor.

Other gp130 ligands such as IL-6 and CNTF have been reported to influence energy metabolism (Febbraio, 2007; Watt et al., 2006). However, the role of CT-1 in fuel homeostasis appears to be unique. At variance with *ct-1*, obesity has not been reported in *cntf* null mice, although CNTF administration causes significant reduction of food intake (Masu et al., 1993).

The effects of IL-6 on energy metabolism remain controversial. While some reports showed that *il-6* null mice were hyperphagic and developed mature-onset obesity (Wallenius et al., 2002), other investigators did not observe obesity or abnormal lipid metabolism in those animals (Di Gregorio et al., 2004). In contrast to other deficiencies of gp130 ligands, *ct-1* null mice represent a model of hypophagic obesity. In these animals excessive weight gain takes place in the presence of reduced food intake, possibly as a result of decreased EE. Although the cause of anorexia in these animals should be further investigated, it may be a compensatory mechanism to slow down excessive weight gain as result of low EE. Neither alterations in physical activity nor thermogenesis seems to account for the low EE observed in *ct-1* null mice under baseline conditions, the more obvious candidate being the reduced metabolic rate. Nevertheless, the underlying biochemical/molecular mechanisms remain to be elucidated. A striking feature of mature *ct-1*$^{-/-}$ mice is the presence of a high RQ, indicative of impaired fat utilization. It has been reported that increased lipid availability observed in obesity enhances the capacity of muscle for fat oxidation (Hancock et al., 2008; Turner et al., 2007). However, in obese *ct-1* null mice (12 months old), fatty acid oxidation was similar to age-matched WT animals, suggesting an impaired capacity to adjust fat oxidation to increased fat mass. Along these lines, *ct-1*$^{-/-}$ young animals were more prone to develop obesity and dyslipidemia than WT mice under the same obesogenic environment, confirming the difficulty of *ct-1*-deficient mice to buffer the excess of dietary fat availability from the early ages of life.

While insulin resistance and type 2 diabetes are found in old obese *ct-1*-deficient mice, young nonobese *ct-1*$^{-/-}$ animals manifest normal insulin sensitivity. This is similar to what is observed in *il-6* knockout mice in which insulin resistance appears to be secondary to obesity (Wallenius et al., 2002). Together with excessive weight gain, adult *ct-1* null mice also manifest impaired fat mobilization, as reflected by downregulation of lipolytic genes and decreased lipolytic response to β-adrenergic agonists in WAT. These alterations can contribute to accumulation of body fat and may be related to insulin resistance (Jocken et al., 2007; Villena et al., 2004). Moreover, adipocytes from mature obese *ct-1* null mice have low mitochondrial DNA content and diminished oxygen consumption together with reduced expression of critical genes influencing mitochondrial biogenesis such as *PGC-1α* and *eNOS*. These alterations are in keeping with reports showing defective mitochondrial content in WAT in both genetic and fat-induced obesity (Rong et al., 2007). The fact that adipocytes from young *ct-1*$^{-/-}$ mice did not exhibit any of the aforementioned disturbances suggests that they are a consequence of obesity. However, we cannot totally rule out that the lack of CT-1 can contribute to aggravate these changes.

The impact of CT-1 deficiency on energy homeostasis prompted us to analyze the metabolic effects of rCT-1 administration. Pharmacological doses of rCT-1 caused a marked reduction of body weight not only in *ct-1*-deficient mice but also in WT lean and diet-induced-obese mice. This effect was leptin independent, as was also found in *ob/ob* mice. The antiobesity properties of rCT-1 were related to the anorexigenic activity of the cytokine and to its ability to increase EE. Similarly to leptin and CNTF (Cota et al., 2006, 2008), rCT-1 induces hypophagia by stimulating hypothalamic STAT-3 and S6 phosphorylation. Also, rCT1 shares with leptin and CNTF the property to increase EE, but the underlying mechanism appears to be different, as these two cytokines, but not rCT-1, upregulate UCP1 in BAT (Blüher et al., 2004; Rouru et al., 1999). In contrast with the lack of effect of rCT-1 on BAT, this cytokine exerts a dramatic remodeling of WAT associated with decreased fat mass. In WT mice reduction of adipocyte size was accompanied by downregulation of lipogenic genes and upregulation of genes involved in lipolysis and fatty acid oxidation. Also, rCT-1 upregulates *UCP2* and genes controlling mitochondrial biogenesis (*TFAM*, *NRF1*, and *eNOS*) together with an elevation in the expression of mtDNA-encoded protein COX1 and an increase in mitochondrial mass and oxygen consumption by isolated adipocytes. These changes in WAT are associated with increased FFA oxidation and upregulation of genes that typify BAT phenotype such as *UCP1*, *PRDM16*, and *Dio2* (Seale et al., 2007). Similar changes are observed in gonadal and subcutaneous WAT from rCT-1-treated *ob/ob* mice. Analogous metabolic remodeling of adipocytes has been described for CNTF. However, there are some important differences between CNTF and CT-1. CNTF does not upregulate *UCP1* in WAT, despite increasing *PGC1α* mRNA, suggesting that CNTF induces mitochondrial biogenesis in adipose tissue but does not enhance the capacity for uncoupled respiration (Crowe et al., 2008). Importantly, rCT-1 is able to directly upregulate *UCP1* and *Dio2* in cultured adipocytes, while CNTF has no comparable effect on these genes, indicating nonredundancy in the biological activities of these two cytokines. All these findings reveal that CT-1 can activate fat utilization in WAT, which might explain the adipose-tissue-lowering effect of this cytokine (Hoehn et al., 2010).

Interestingly, we found that rCT-1 administration decreases both fasting and postprandial RQ, causes a rapid clearance of FFA from plasma after a lipid load, reduces postprandial hypertriglyceridemia, upregulates genes involved in FFA oxidation in muscle, and increases the ability of skeletal muscle to oxidize palmitate. These data show that CT-1, in addition to promoting fat utilization in WAT, boosts FFA oxidation in muscle. AMPK is considered to be a master switch in the regulation of lipid metabolism, and its activation stimulates mitochondrial biogenesis and fatty acid oxidation in muscle (Hardie, 2008; Viollet et al., 2003). Our data demonstrate that rCT-1 activates AMPK in muscle and that AMPKα2 mediates the stimulatory effect of CT-1 on fatty acid oxidation, as has also been reported for leptin and CNTF (Minokoshi et al., 2002; Watt et al., 2006). The mechanisms by which rCT-1 activates AMPK remain to be defined but will be critical for our understanding of rCT-1 signaling in skeletal muscle.

In humans with the metabolic syndrome, serum CT-1 levels are increased, and it has been proposed that this cytokine might cause insulin resistance (Natal et al., 2008). In contrast with this view, our data indicate that CT-1 displays glucose-lowering activity. This concept is supported by the following findings: (1) rCT-1 activates AKT in muscle, (2) pretreatment of mice with rCT-1 enhances insulin-induced AKT activation in skeletal muscle, (3) in vitro incubation of L6E9 myocytes with rCT-1 increases insulin-mediated AKT phosphorylation and glucose uptake, (4) administration of rCT-1 reduces glycemia after a sugar-rich meal, and (5) rCT-1 corrects hyperglycemia in STZ-treated insulin-deficient mice, an effect that is remarkable,

as it indicates that rCT-1 is capable of promoting glucose utilization independently of insulin. In consonance with these effects, chronic administration of rCT-1 is able to reverse insulin resistance in obese mice. It seems possible that the ability of CT-1 to enhance FFA oxidation may contribute to its insulin-sensitizing properties, since high levels of FFA have been suggested to cause insulin resistance in all major insulin target organs (Boden, 2008). Importantly, rCT-1 enhances insulin signaling in muscle, and it should be noted that the muscle is the largest insulin-sensitive tissue that contributes up to 90% of the insulin-stimulated glucose disposal in healthy individuals (Kristiansen and Mandrup-Poulsen, 2005). This property is shared with CNTF (Watt et al., 2006), while the role of IL-6 on insulin sensitivity remains controversial (Kristiansen and Mandrup-Poulsen, 2005). With respect to the interaction of CT-1 and insulin in adipose tissue, our data both in vivo (Figure 4) and in vitro (Figure S4) argue against the hypothesis that CT-1 may be a mediator of impaired insulin signaling in adipocytes, as previously suggested (Zvonic et al., 2004).

CT-1 has already been shown to possess cytoprotective and hypotensor properties (Calabrò et al., 2009). According to these data and to the metabolic effects described for CT-1 in this paper, we may hypothesize that the reported overproduction of CT-1 in obese subjects with metabolic syndrome (Natal et al., 2008), hypertension (Pemberton et al., 2005), and coronary artery disease (Talwar et al., 2001) could be a protective mechanism to counteract the emergence of obesity-related disorders such as type 2 diabetes or cardiovascular dysfunctions. Indeed, our data point to CT-1 as a promising therapy for obesity and linked metabolic disorders. This is not only because CT-1 activates fat utilization and improves glucose homeostasis but also because it possesses anorexigenic properties. Nevertheless, it should be considered that chronic administration of CT-1 has been shown to promote heart hypertrophy and myocardium remodeling in mice (Bordet et al., 1999; Pennica et al., 1995). On the other hand, cytokines of the gp130 family might induce inflammatory responses. However, we found neither signs of cardiac toxicity, nor manifestations of systemic inflammatory reaction in mice treated with rCT-1 for 6–10 days at the doses used in this study. Therefore, there are grounds for hope that CT-1 might represent a promising therapeutic agent of utility in the metabolic syndrome.

EXPERIMENTAL PROCEDURES

Animals

ct-1 null mice were generated as described by Oppenheim et al. (2001). We analyzed mice backcrossed into a C57BL/6J background for 11 generations (provided by Diane Pennica, Genentech, and Bettina Holtmann, University of Wuerzburg, Germany). C57BL/6J mice were originally obtained from The Jackson Laboratory (Bar Harbor, ME). *AMPKα2*$^{-/-}$ were generated as described (Viollet et al., 2003) and used at 8 weeks of age. All experimental procedures were approved by the University of Navarra Ethics Committee.

Body Composition Analysis

Whole animal body composition was measured in live conscious animals using QMR technology (EchoMRI-100-700, Echo Medical Systems, Houston, TX).

Food Intake, Indirect Calorimetry, and Locomotor Activity

Body weight and food intake were measured three times per week in WT and *ct-1*$^{-/-}$ mice from 2 to 12 months old. EE was measured by indirect calorimetry. Oxygen consumption (VO_2) and carbon dioxide production (VCO_2) were measured using the Oxylet System (Panlab, Spain), which was also used for continuous recording of locomotor activity through extensiometric weight transducers placed below the home cage.

Treatments with rCT-1

Chronic effects of rCT-1 (6 or 10 days therapy) were evaluated in different experimental models fed with NCD or HFD as well as in *ob/ob* mice. We also determined the acute effects of rCT-1 on postprandial lipemia and glycemia in normal mice and on glucose metabolism in STZ-induced diabetic mice (see Supplemental Experimental Procedures).

Biochemistry

All serum measurements were done on mice fasted for 16 hr, unless otherwise indicated, using a Cobas Mira Autoanalyzer (Roche Diagnostic, Basel, Switzerland) (see Supplemental Experimental Procedures).

Sensitivity to Insulin

Insulin sensitivity was evaluated by ITT and insulin signaling (see Supplemental Experimental Procedures).

Lipolysis

We performed ex vivo lipolysis in adipocytes isolated from epididymal fat. Isolated adipocytes were incubated in Krebs-Ringer HEPES buffer with or without 10^{-6} M isoproterenol during 90 min at 37°C. Lipolysis was evaluated by the determination of the amount glycerol released into the media.

Adipocyte Oxygen Consumption, Mitochondrial Content, and Mitochondrial DNA

Adipocytes were isolated from epididymal fat, and oxygen consumption was measured in a BD Oxygen Biosensor System plate (BD Biosciences) as previously described (Wilson-Fritch et al., 2004). Mitochondrial mass was determined in isolated adipocytes using MitoTracker Green FM (Molecular Probes, Invitrogen). Total DNA was extracted from epididymal fat using QIAamp DNA kit (QIAGEN), and mtDNA was calculated using real-time quantitative PCR as previously described (Bonnard et al., 2008).

Histological Analysis

Sections of paraffin-embedded tissues were stained with H&E. Adipocyte cell size was determined using Matlab 7.1.0.83 R14 (SP13) and diplid 1.6 (http://www.diplib.org/) software. At least 300 cells from each sample were measured.

Palmitate Oxidation in Muscle and Adipose Tissue

Palmitate oxidation was determined in fragments of adipose tissue and muscle strips as described (Hoehn et al., 2010) (see Supplemental Experimental Procedures).

Real-Time Quantitative PCR, Protein Extraction, and Western Blotting

See Supplemental Experimental Procedures.

2-Deoxy-D-[^{3}H]Glucose Uptake in Cells and Isolated Soleus Muscle

L6E9 rat skeletal muscle cell line and 3T3-L1 adipocytes were grown, and 2-deoxy-d-[^{3}H]glucose uptake was performed as previously reported (Suárez et al., 2001). 2DG uptake was also determined in muscle strips as described (Dray et al., 2008) (see Supplemental Experimental Procedures).

Statistical Analyses

Results are expressed as the mean ± SEM. Statistical analyses were conducted using the GraphPad Prism software version 4.00 for Windows (GraphPad Software). Data were tested for normality and subjected to t tests or one-way ANOVA with Tukey's posttest, unless otherwise indicated. The adipocyte size distribution was analyzed by the Wilcoxon signed-rank test.

SUPPLEMENTAL INFORMATION

Supplemental Information includes Supplemental Experimental Procedures, five figures, three tables, and Supplemental References and can be found with this article online at doi:10.1016/j.cmet.2011.05.013.

ACKNOWLEDGMENTS

This work was supported by agreement between FIMA and the "UTE project CIMA" and by grant FIS PI041321 (M.B.), grant Mutua Madrileña (M.B.), a grant from the Department of Health of Gobierno de Navarra (M.J.M.-A. and M.B.), and Línea Especial "Nutrición, Obesidad y Salud" Universidad de Navarra (J.A.M., M.J.M.-A., and B.M.-G.). N.P.-E. was supported by the National Research Program Torres Quevedo. We thank Diane Pennica (Genentech) and Bettina Holtmann (University of Wuerzburg, Germany) for providing the *ct-1* null mice and Fundación Pedro Barrie de la Maza y Condesa de Fenosa and Fundación Echebano for financial support. We thank Dr. Fernández-Trocóniz, University of Navarra, for performing the pharmacokinetic analysis of rCT-1 in mice and for helpful discussion. We also thank I. Belza, C. Méndez, M. Zabala, A. Lorente, and V. Ciaurriz for technical support. This manuscript was also improved by comments from the anonymous reviewers. M.B. and J.P. share senior authorship.

Received: January 12, 2010
Revised: February 23, 2011
Accepted: May 18, 2011
Published: August 2, 2011

REFERENCES

Blüher, S., Moschos, S., Bullen, J., Jr., Kokkotou, E., Maratos-Flier, E., Wiegand, S.J., Sleeman, M.W., and Mantzoros, C.S. (2004). Ciliary neurotrophic factorAx15 alters energy homeostasis, decreases body weight, and improves metabolic control in diet-induced obese and UCP1-DTA mice. Diabetes *53*, 2787–2796.

Boden, G. (2008). Obesity and free fatty acids. Endocrinol. Metab. Clin. North Am. *37*, 635–646, viii–ix.

Bonnard, C., Durand, A., Peyrol, S., Chanseaume, E., Chauvin, M.A., Morio, B., Vidal, H., and Rieusset, J. (2008). Mitochondrial dysfunction results from oxidative stress in the skeletal muscle of diet-induced insulin-resistant mice. J. Clin. Invest. *118*, 789–800.

Bordet, T., Schmalbruch, H., Pettmann, B., Hagege, A., Castelnau-Ptakhine, L., Kahn, A., and Haase, G. (1999). Adenoviral cardiotrophin-1 gene transfer protects pmn mice from progressive motor neuronopathy. J. Clin. Invest. *104*, 1077–1085.

Bustos, M., Beraza, N., Lasarte, J.J., Baixeras, E., Alzuguren, P., Bordet, T., and Prieto, J. (2003). Protection against liver damage by cardiotrophin-1: a hepatocyte survival factor up-regulated in the regenerating liver in rats. Gastroenterology *125*, 192–201.

Calabrò, P., Limongelli, G., Riegler, L., Maddaloni, V., Palmieri, R., Golia, E., Roselli, T., Masarone, D., Pacileo, G., Golino, P., and Calabrò, R. (2009). Novel insights into the role of cardiotrophin-1 in cardiovascular diseases. J. Mol. Cell. Cardiol. *46*, 142–148.

Cota, D., Proulx, K., Smith, K.A., Kozma, S.C., Thomas, G., Woods, S.C., and Seeley, R.J. (2006). Hypothalamic mTOR signaling regulates food intake. Science *312*, 927–930.

Cota, D., Matter, E.K., Woods, S.C., and Seeley, R.J. (2008). The role of hypothalamic mammalian target of rapamycin complex 1 signaling in diet-induced obesity. J. Neurosci. *28*, 7202–7208.

Crowe, S., Turpin, S.M., Ke, F., Kemp, B.E., and Watt, M.J. (2008). Metabolic remodeling in adipocytes promotes ciliary neurotrophic factor-mediated fat loss in obesity. Endocrinology *149*, 2546–2556.

Di Gregorio, G.B., Hensley, L., Lu, T., Ranganathan, G., and Kern, P.A. (2004). Lipid and carbohydrate metabolism in mice with a targeted mutation in the IL-6 gene: absence of development of age-related obesity. Am. J. Physiol. Endocrinol. Metab. *287*, E182–E187.

Dray, C., Knauf, C., Daviaud, D., Waget, A., Boucher, J., Buléon, M., Cani, P.D., Attané, C., Guigné, C., Carpéné, C., et al. (2008). Apelin stimulates glucose utilization in normal and obese insulin-resistant mice. Cell Metab. *8*, 437–445.

Febbraio, M.A. (2007). gp130 receptor ligands as potential therapeutic targets for obesity. J. Clin. Invest. *117*, 841–849.

Febbraio, M.A., Hiscock, N., Sacchetti, M., Fischer, C.P., and Pedersen, B.K. (2004). Interleukin-6 is a novel factor mediating glucose homeostasis during skeletal muscle contraction. Diabetes *53*, 1643–1648.

Hancock, C.R., Han, D.H., Chen, M., Terada, S., Yasuda, T., Wright, D.C., and Holloszy, J.O. (2008). High-fat diets cause insulin resistance despite an increase in muscle mitochondria. Proc. Natl. Acad. Sci. USA *105*, 7815–7820.

Hardie, D.G. (2008). AMPK: a key regulator of energy balance in the single cell and the whole organism. Int. J. Obes. (Lond.) *32* (*Suppl 4*), S7–S12.

Hiscock, N., Chan, M.H., Bisucci, T., Darby, I.A., and Febbraio, M.A. (2004). Skeletal myocytes are a source of interleukin-6 mRNA expression and protein release during contraction: evidence of fiber type specificity. FASEB J. *18*, 992–994.

Hoehn, K.L., Turner, N., Swarbrick, M.M., Wilks, D., Preston, E., Phua, Y., Joshi, H., Furler, S.M., Larance, M., Hegarty, B.D., et al. (2010). Acute or chronic upregulation of mitochondrial fatty acid oxidation has no net effect on whole-body energy expenditure or adiposity. Cell Metab. *11*, 70–76.

Iñiguez, M., Berasain, C., Martinez-Ansó, E., Bustos, M., Fortes, P., Pennica, D., Avila, M.A., and Prieto, J. (2006). Cardiotrophin-1 defends the liver against ischemia-reperfusion injury and mediates the protective effect of ischemic preconditioning. J. Exp. Med. *203*, 2809–2815.

Janoschek, R., Plum, L., Koch, L., Münzberg, H., Diano, S., Shanabrough, M., Müller, W., Horvath, T.L., and Brüning, J.C. (2006). gp130 signaling in proopiomelanocortin neurons mediates the acute anorectic response to centrally applied ciliary neurotrophic factor. Proc. Natl. Acad. Sci. USA *103*, 10707–10712.

Jocken, J.W., Langin, D., Smit, E., Saris, W.H., Valle, C., Hul, G.B., Holm, C., Arner, P., and Blaak, E.E. (2007). Adipose triglyceride lipase and hormone-sensitive lipase protein expression is decreased in the obese insulin-resistant state. J. Clin. Endocrinol. Metab. *92*, 2292–2299.

Kristiansen, O.P., and Mandrup-Poulsen, T. (2005). Interleukin-6 and diabetes: the good, the bad, or the indifferent? Diabetes *54* (*Suppl 2*), S114–S124.

Lambert, P.D., Anderson, K.D., Sleeman, M.W., Wong, V., Tan, J., Hijarunguru, A., Corcoran, T.L., Murray, J.D., Thabet, K.E., Yancopoulos, G.D., and Wiegand, S.J. (2001). Ciliary neurotrophic factor activates leptin-like pathways and reduces body fat, without cachexia or rebound weight gain, even in leptin-resistant obesity. Proc. Natl. Acad. Sci. USA *98*, 4652–4657.

Marquès, J.M., Belza, I., Holtmann, B., Pennica, D., Prieto, J., and Bustos, M. (2007). Cardiotrophin-1 is an essential factor in the natural defense of the liver against apoptosis. Hepatology *45*, 639–648.

Masu, Y., Wolf, E., Holtmann, B., Sendtner, M., Brem, G., and Thoenen, H. (1993). Disruption of the CNTF gene results in motor neuron degeneration. Nature *365*, 27–32.

Minokoshi, Y., Kim, Y.B., Peroni, O.D., Fryer, L.G., Müller, C., Carling, D., and Kahn, B.B. (2002). Leptin stimulates fatty-acid oxidation by activating AMP-activated protein kinase. Nature *415*, 339–343.

Natal, C., Fortuño, M.A., Restituto, P., Bazán, A., Colina, I., Díez, J., and Varo, N. (2008). Cardiotrophin-1 is expressed in adipose tissue and upregulated in the metabolic syndrome. Am. J. Physiol. Endocrinol. Metab. *294*, E52–E60.

Oppenheim, R.W., Wiese, S., Prevette, D., Armanini, M., Wang, S., Houenou, L.J., Holtmann, B., Gotz, R., Pennica, D., and Sendtner, M. (2001). Cardiotrophin-1, a muscle-derived cytokine, is required for the survival of subpopulations of developing motoneurons. J. Neurosci. *21*, 1283–1291.

Pemberton, C.J., Raudsepp, S.D., Yandle, T.G., Cameron, V.A., and Richards, A.M. (2005). Plasma cardiotrophin-1 is elevated in human hypertension and stimulated by ventricular stretch. Cardiovasc. Res. *68*, 109–117.

Pennica, D., Arce, V., Swanson, T.A., Vejsada, R., Pollock, R.A., Armanini, M., Dudley, K., Phillips, H.S., Rosenthal, A., Kato, A.C., and Henderson, C.E. (1996). Cardiotrophin-1, a cytokine present in embryonic muscle, supports long-term survival of spinal motoneurons. Neuron *17*, 63–74.

Pennica, D., King, K.L., Shaw, K.J., Luis, E., Rullamas, J., Luoh, S.M., Darbonne, W.C., Knutzon, D.S., Yen, R., Chien, K.R., et al. (1995). Expression cloning of cardiotrophin 1, a cytokine that induces cardiac myocyte hypertrophy. Proc. Natl. Acad. Sci. USA *92*, 1142–1146.

Rong, J.X., Qiu, Y., Hansen, M.K., Zhu, L., Zhang, V., Xie, M., Okamoto, Y., Mattie, M.D., Higashiyama, H., Asano, S., et al. (2007). Adipose mitochondrial biogenesis is suppressed in db/db and high-fat diet-fed mice and improved by rosiglitazone. Diabetes *56*, 1751–1760.

Rouru, J., Cusin, I., Zakrzewska, K.E., Jeanrenaud, B., and Rohner-Jeanrenaud, F. (1999). Effects of intravenously infused leptin on insulin sensitivity and on the expression of uncoupling proteins in brown adipose tissue. Endocrinology *140*, 3688–3692.

Seale, P., Kajimura, S., Yang, W., Chin, S., Rohas, L.M., Uldry, M., Tavernier, G., Langin, D., and Spiegelman, B.M. (2007). Transcriptional control of brown fat determination by PRDM16. Cell Metab. *6*, 38–54.

Steensberg, A., van Hall, G., Osada, T., Sacchetti, M., Saltin, B., and Klarlund Pedersen, B. (2000). Production of interleukin-6 in contracting human skeletal muscles can account for the exercise-induced increase in plasma interleukin-6. J. Physiol. *529*, 237–242.

Steinberg, G.R., Watt, M.J., Fam, B.C., Proietto, J., Andrikopoulos, S., Allen, A.M., Febbraio, M.A., and Kemp, B.E. (2006). Ciliary neurotrophic factor suppresses hypothalamic AMP-kinase signaling in leptin-resistant obese mice. Endocrinology *147*, 3906–3914.

Suárez, E., Bach, D., Cadefau, J., Palacin, M., Zorzano, A., and Gumá, A. (2001). A novel role of neuregulin in skeletal muscle. Neuregulin stimulates glucose uptake, glucose transporter translocation, and transporter expression in muscle cells. J. Biol. Chem. *276*, 18257–18264.

Talwar, S., Downie, P.F., Squire, I.B., Davies, J.E., Barnett, D.B., and Ng, L.L. (2001). Plasma N-terminal pro BNP and cardiotrophin-1 are elevated in aortic stenosis. Eur. J. Heart Fail. *3*, 15–19.

Tilg, H., and Moschen, A.R. (2006). Adipocytokines: mediators linking adipose tissue, inflammation and immunity. Nat. Rev. Immunol. *6*, 772–783.

Turner, N., Bruce, C.R., Beale, S.M., Hoehn, K.L., So, T., Rolph, M.S., and Cooney, G.J. (2007). Excess lipid availability increases mitochondrial fatty acid oxidative capacity in muscle: evidence against a role for reduced fatty acid oxidation in lipid-induced insulin resistance in rodents. Diabetes *56*, 2085–2092.

Villena, J.A., Roy, S., Sarkadi-Nagy, E., Kim, K.H., and Sul, H.S. (2004). Desnutrin, an adipocyte gene encoding a novel patatin domain-containing protein, is induced by fasting and glucocorticoids: ectopic expression of desnutrin increases triglyceride hydrolysis. J. Biol. Chem. *279*, 47066–47075.

Viollet, B., Andreelli, F., Jørgensen, S.B., Perrin, C., Geloen, A., Flamez, D., Mu, J., Lenzner, C., Baud, O., Bennoun, M., et al. (2003). The AMP-activated protein kinase alpha2 catalytic subunit controls whole-body insulin sensitivity. J. Clin. Invest. *111*, 91–98.

Viollet, B., Athea, Y., Mounier, R., Guigas, B., Zarrinpashneh, E., Horman, S., Lantier, L., Hebrard, S., Devin-Leclerc, J., Beauloye, C., et al. (2009). AMPK: Lessons from transgenic and knockout animals. Front. Biosci. *14*, 19–44.

Wallenius, V., Wallenius, K., Ahrén, B., Rudling, M., Carlsten, H., Dickson, S.L., Ohlsson, C., and Jansson, J.O. (2002). Interleukin-6-deficient mice develop mature-onset obesity. Nat. Med. *8*, 75–79.

Watt, M.J., Dzamko, N., Thomas, W.G., Rose-John, S., Ernst, M., Carling, D., Kemp, B.E., Febbraio, M.A., and Steinberg, G.R. (2006). CNTF reverses obesity-induced insulin resistance by activating skeletal muscle AMPK. Nat. Med. *12*, 541–548.

Wilson-Fritch, L., Nicoloro, S., Chouinard, M., Lazar, M.A., Chui, P.C., Leszyk, J., Straubhaar, J., Czech, M.P., and Corvera, S. (2004). Mitochondrial remodeling in adipose tissue associated with obesity and treatment with rosiglitazone. J. Clin. Invest. *114*, 1281–1289.

Wojtaszewski, J.F., Jørgensen, S.B., Hellsten, Y., Hardie, D.G., and Richter, E.A. (2002). Glycogen-dependent effects of 5-aminoimidazole-4-carboxamide (AICA)-riboside on AMP-activated protein kinase and glycogen synthase activities in rat skeletal muscle. Diabetes *51*, 284–292.

Wojtaszewski, J.F., and Richter, E.A. (2006). Effects of acute exercise and training on insulin action and sensitivity: focus on molecular mechanisms in muscle. Essays Biochem. *42*, 31–46.

Wueest, S., Rapold, R.A., Rytka, J.M., Schoenle, E.J., and Konrad, D. (2009). Basal lipolysis, not the degree of insulin resistance, differentiates large from small isolated adipocytes in high-fat fed mice. Diabetologia *52*, 541–546.

Zvonic, S., Hogan, J.C., Arbour-Reily, P., Mynatt, R.L., and Stephens, J.M. (2004). Effects of cardiotrophin on adipocytes. J. Biol. Chem. *279*, 47572–47579.